

Enhancing decision-making for climate change mitigation and sustainable urban growth

Zahra Parvar, Marjan Mohammadzadeh*, Sepideh Saeidi

Department of Environmental Sciences, Faculty of Fisheries and Environmental Sciences, Gorgan University of Agricultural Sciences and Natural Resources, Gorgan, Golestan, Iran



ARTICLE INFO

Keywords:
 SLEUTH model
 Land surface temperature
 InVEST model
 Green space suitability
 Landscape metrics

ABSTRACT

Uncontrolled urban expansion presents significant challenges to green spaces, leading to increased land surface temperature, and carbon emissions. This study emphasizes the importance of predicting urban growth, monitoring LST, and assessing green space suitability to mitigate these impacts in Bojnourd City, Iran. This research aims to enhance land use planning by employing the SLEUTH model and integrating landscape features to evaluate and compare urban growth scenarios. The study consisted of five main stages: monitoring LULC and LST changes, utilizing the InVEST Carbon Storage and Sequestration model for carbon stock mapping, assessing green space suitability, simulating urban growth scenarios up to 2050, and prioritizing scenarios using landscape metrics and TOPSIS. Five scenarios were analyzed: Low Carbon City, Compact Urban Growth, Historical Urban Growth, Uncontrolled Urban Growth, and Green City. Landscape metrics were utilized to assess the environmental consequences of each scenario. The results demonstrate that the Compact Urban Growth scenario, which focuses on land conservation, achieved the highest environmental sustainability score of 0.818, followed by the Green City scenario at 0.72, and the Low Carbon City scenario at 0.55. These findings highlight the effectiveness of the SLEUTH model in guiding urban planners toward decisions that promote sustainable, low-carbon urban development.

1. Introduction

The ongoing interaction between human activities and urbanization has a profound impact on the natural environment. This interaction is leading to rapid changes in the composition of land (Kumar, 2018; Pham and Lin, 2023; Unal Cilek and Cilek, 2021). These alterations in land composition, affect the dynamics of the Earth's surface, impacting ecosystem services and environmental quality (Li et al., 2018a). Urban areas significantly contribute to carbon emissions (Varquez et al., 2023; Yeh et al., 2021; Zhao et al., 2023), affecting ecosystem services, biological diversity and regional environments, leading to adverse impacts on climate variability and the environment (Azmi et al., 2021; Han et al., 2023). Unplanned and irregular expansion in peri-urban lands is emphasized as a primary concern that demands the attention of managers and urban planners across various administrative levels (Falah et al., 2020). One negative outcome of urbanization is the encroachment of urban development on agricultural and natural areas, leading to their decline (Kazemi and Hosseinpour, 2022). The replacement of green spaces with impervious surfaces results in the loss of carbon storage and disrupts carbon sequestration, ultimately leading to increased carbon emissions (X. Liu et al., 2024). The presence of

* Corresponding author.

E-mail addresses: Mohammadzadeh@gau.ac.ir (M. Mohammadzadeh), s.saeidi@gau.ac.ir (S. Saeidi).

carbon sinks in urban and peri-urban areas is contributing to the mitigation of the global greenhouse gas impact (Ariluoma et al., 2021; Hwang et al., 2022). Urban green spaces (UGS) (Bai et al., 2018; Cheng et al., 2021; Qiao et al., 2022; Stumpe et al., 2023) and peri-urban green spaces (P-UGS) are crucial for climate resilience and mitigation (Fusaro et al., 2015; Stumpe et al., 2023; Sun and Shao, 2020; Verdú-Vázquez et al., 2021; Zlender and Ward Thompson, 2017). They reduce greenhouse gas emissions, provide carbon sequestration, and cool local environments through shading, making them essential for effective land use planning (Ariluoma et al., 2021; Kafy et al., 2023). Understanding the thermal environment in urban and peri-urban areas is essential for enhancing urban planning and devising strategies to handle urban thermal loads effectively (Han et al., 2022). Assessing urban thermal environments involves using remote sensing to measure land surface temperature (LST) and analyze urban development's impact on local thermal climates (Parvar et al., 2024a). Cities are central to efforts aimed at adjusting and responding to global climate change (Alavipanah et al., 2018). Preventing irrational urban expansion is effectively achieved by implementing an urban development boundary, which aims to protect green spaces and agricultural lands from occupation (J. Liu et al., 2017). In this context, assessment, prediction, and evaluation of land-use dynamics, encompassing both quantitative and qualitative aspects, have assumed a pivotal role in the domain of land-system science, with a particular focus on urban science (Rienow and Goetzke, 2015b). The process entails the selection of suitable land development policies, which comes after a meticulous examination of various urban growth scenarios. Simulation models are then employed to simulate built-up land densities corresponding to different developmental options (Saxena et al., 2021).

Urban remote sensing and modeling are critical for evaluating and forecasting urban growth (Saxena and Jat, 2019). SLEUTH, a widely-used bottom-up Cellular Automata (CA) approach, simulates urban growth by predicting trends from historical data, providing more reliable results with recent input data for regions with medium to slow development rates (Chaudhuri and Clarke, 2019; Dietzel and Clarke, 2006; Rafiee et al., 2009). To improve the simulation of urban growth, integrating SLEUTH with other models, such as the InVEST model (Adelisardou et al., 2022; J. Liu et al., 2017; Zarandian et al., 2023), Multi Criteria Evaluation (MCE) (A. Mahiny and Clarke, 2013; A. S. Mahiny and Clarke, 2012; Mahiny and Gholamalifard, 2011; Parvar et al., 2024b; Saeidi et al., 2018; Yin et al., 2016), analytical hierarchical process (AHP) (Aburas et al., 2017; Martellozzo et al., 2018), logistic regression (LR) (Jafari et al., 2016; Ozdemir, 2011), support vector machine (Rienow and Goetzke, 2015a; Yang et al., 2008), random forest (Gounaridis et al., 2019), artificial neural network (Liang et al., 2018) is recommended.

Li et al. (2020) demonstrated the power of integrating the SLEUTH and InVEST models to simulate urban growth, highlighting how integrated spatial regulation can better promote regional sustainable development compared to traditional methods (Li et al., 2020). Saxena and Jat (2019) introduced a groundbreaking approach by integrating land suitability into SLEUTH-based urban growth modeling, significantly improving prediction accuracy. This innovative method effectively connects land suitability assessments with urban development dynamics, representing a critical advancement in the field (Mohammadyari et al., 2023). Accurately forecasting urban land expansion is crucial for informing policymakers. Integrating scenario prediction techniques not only improves our understanding of future scenarios but also enables decision-makers to strategize for long-term sustainability (Feng et al., 2012; Liu et al., 2020a). Historically, urban growth models have focused primarily on historical and spatial data, often overlooking land suitability assessments. This research follows a paradigm shift in urban planning, by setting limits for urban development and establishing ecological boundaries, it offers a proactive approach to mitigate urban sprawl and safeguard natural resources.

This research aims to enhance land use planning by employing the SLEUTH model and integrating landscape features with The Technique for Order of Preference by Similarity to Ideal Solution (TOPSIS) to evaluate and compare urban growth scenarios. It tackles the challenges of uncontrolled urban growth and the effective demarcation of urban boundaries. The study emphasizes the critical roles of green spaces in temperature regulation, carbon sequestration, and urban expansion control. It highlights the benefits of GS

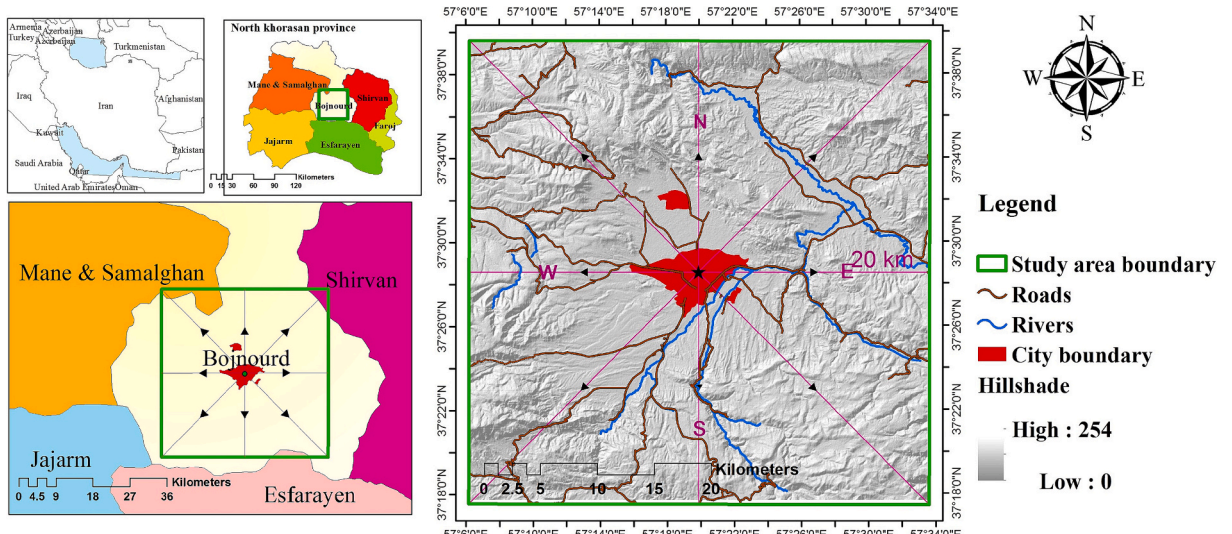


Fig. 1. Study area.

suitability maps and carbon sequestration models in identifying high-value green areas. By adjusting coefficients and incorporating supplementary layers, the SLEUTH model supports diverse urban growth scenarios. Additionally, by promoting the conservation and strategic placement of green spaces, this research may contribute to mitigating global warming through enhanced carbon sequestration and temperature regulation.

2. Materials and method

2.1. Study area

Case studies are important for testing and developing theories in real-world situations (Parvar et al., 2024a). This study focuses on Bojnourd, the capital city of North Khorasan Province in northeastern Iran. Bojnourd has experienced rapid growth since 2013 due to political and economic changes. The study area covers 1640 km² and includes both urban and rural landscapes surrounding Bojnourd City in the North Khorasan province of Iran (Fig. 1).

2.2. Data and meteorological

Remote sensing data, including multi-temporal Landsat satellite images (Collection 2 Tier 1 Level 2) with minimal cloud cover (< 5 %) and a spatial resolution of 30 m, were employed to generate Land Surface Temperature (LST) and Land Use Land Cover (LULC) maps from 1989 to 2021. To extract topographical details such as elevation, slope, and aspect, the DEM ALOS World 3D - 30 m was employed.

2.3. Methodology

The research consisted of five main stages:

1. Monitoring changes in LULC and LST.
2. Using the InVEST - Carbon Storage and Sequestration (CSS) model.
3. Evaluating the suitability of Green Spaces (GS).
4. Simulating urban growth scenarios.
5. Prioritizing scenarios by utilizing landscape metrics.

Fig. 2 illustrates the research procedure, providing detailed information about each step.

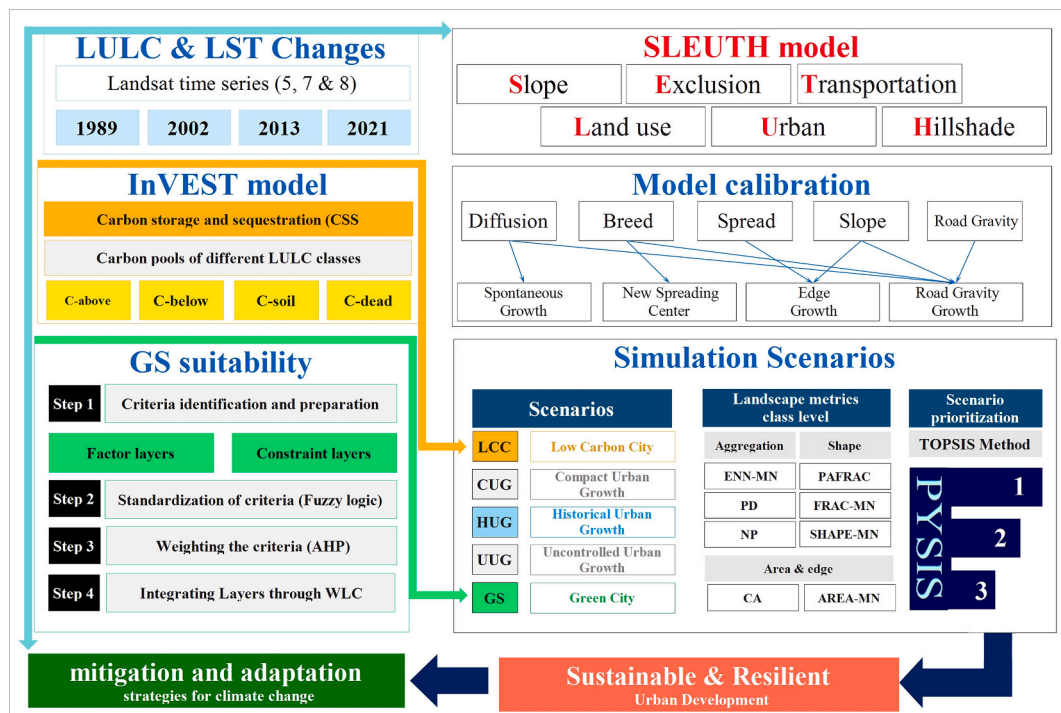


Fig. 2. The overall research flowchart.

2.3.1. Monitoring changes in LULC and LST

LULC changes: The preparation of LULC maps is a critical process that serves as the foundation for subsequent analyses (Rwanga and Ndambuki, 2017). In this study, LULC maps were created using Decision Tree Classification (DTC) with ENVI 5.3 software, employing a combination of supervised and unsupervised methods. The Normalized Difference Built-up Index (NDBI) and Normalized Difference Vegetation Index (NDVI) were utilized for identifying built-up areas and classifying various land cover types (Punia et al., 2011; Rwanga and Ndambuki, 2017). Six classes, including grassland, urban green spaces (UGS), built-up, Road, garden, and agriculture, were considered. For accuracy assessment, 270 reference pixels were collected from high-resolution Landsat images, Google Earth data, and other maps. A confusion matrix evaluated the classification performance, with overall accuracy calculated as the ratio of correctly classified pixels to the total reference pixels. Producer and user accuracy metrics assessed correct classifications and misclassifications, while the Kappa coefficient indicated agreement between the classified map and reference data, ranging from 0 (random agreement) to 1 (perfect agreement) (Imen et al., 2022; Pal and Ziaul, 2017).

LST trend: Understanding the dynamics of LST is crucial for gaining insights into its broader impact on regional climates (Parvar and Salmanmahiny, 2024).

The seasonal/annual LST trend spanning from 1989 to 2021 was assessed in Bojnourd city, utilizing the atmospherically corrected Landsat Collection 2 Level 2 Surface Reflectance dataset. This analysis was conducted by implementing a specialized algorithm and equation within the Google Earth Engine (GEE) platform, as detailed in Eq. 1 (Pande et al., 2023):

$$L_\lambda = M_L \cdot MQ_{CAL} + A_L \quad (1)$$

In this context, the variables represent key parameters used in the conversion process from Digital Numbers (DN) to spectral radiance. L_λ stands for spectral radiance, M_L denotes the multiplicative radiance scaling factor, A_L represents the radiance additive scaling factor for the band, and Q_{CAL} signifies the DN value to be converted into radiance.

The relative contribution of each LULC class to the LST was analyzed using the 'Tabulate Area' tool in ArcGIS. This tool allowed us to calculate the thermal impact of each LULC class by quantifying the area of each class within specific temperature ranges, thus providing insights into the thermal environment associated with each land cover type.

2.3.2. Using the InVEST - carbon storage and sequestration (CSS) model

To develop a low-carbon city scenario, the InVEST - CSS model utilized remote sensing data to assess carbon storage and sequestration dynamics. This model, which focuses on carbon storage and sequestration, relies on four main carbon pools for each LULC type: above-ground biomass (C-above), below-ground biomass (C-below), soil organic carbon (C-soil), and dead organic matter (C-dead) (Sharp et al., 2018). Carbon pools for each LULC type were derived from data in the IPCC report (Change, 2006; Eggleston et al., 2006; Sharp et al., 2018) (Table 1).

If local or regional carbon estimates are not available, default values from the IPCC (2006) can be assigned. The sources for estimating carbon storage are as follows (Eggleston et al., 2006; Zhongming et al., 2019):

- Carbon stored in above-ground biomass: Data from Table 4.1 on page 4.46 and Tables 5.1 to 5.3 on page 5.9 of the IPCC (2006) report (Change, 2006), along with a digital version of the FAO's environmental map, were utilized.
- Carbon stored in below-ground biomass: Referenced from Table 4.4 on page 4.49 and Table 6.4 on page 6.27 of the IPCC (2006) report.
- Carbon stored in soil: Estimated using Table 2.3 and Tables 5.5 and 6.2 from the IPCC (2006) report.
- Carbon stored in dead organic matter: Values from Table 2.2 on page 2.27 of the IPCC (2006) report were used.

In this research, areas with high carbon sequestration potential were identified and designated as excluded layers within the urban growth scenario. The CSS map was used to constrain urban expansion in the LCC scenario. This approach aims to limit carbon emissions and promote resilience by directing development toward regions more suitable for carbon sequestration.

2.3.3. Evaluating the suitability of green spaces (GS)

In this research, we utilized Multi-Criteria Evaluation (MCE)-Weighted Linear Combination (WLC) method in TerrSet 2020 software to generate a green space (GS) suitability map. The process involved five main steps:

Step 1. Criteria identification and preparation: Criteria for evaluating GS suitability were investigated based on previous research and expert opinions (Table 2).

Table 1

Carbon pools of different LULC classes in the InVEST model (unit: tons of C).

LULC class	LULC code	C-above	C-below	C-soil	C-dead
Road	1	0	0	0	0
Grassland	2	0.76	2.16	19	0
UGS	3	63	16.128	13.68	0.4
Built-Up	4	0	0	0	0
Garden	5	63	16.128	13.68	0.4
Agriculture	6	7.68	1.5	18.81	0

Residential areas and roads were identified as constraints in the suitability analysis.

Step 2. Standardization of criteria maps (Fuzzy logic): Fuzzy logic was employed to standardize criteria and transform them into images on a suitability scale ranging from 0 to 1, addressing uncertainties and system ambiguities (Ahmadi Mirgha et al., 2020; Esmaeilpour-Poodeh et al., 2019).

Step 3. Weighting the criteria (AHP): Criteria weights were assigned using the AHP framework, derived from Saaty's pairwise comparison method, considering expert opinions and parameter significance (Cao et al., 2019; Riveira and Maseda, 2006; Saaty, 1977). The questionnaire was distributed among 15 experts in the fields of land planning, urban planning, and green spaces.

Step 4. Integrating Layers through WLC: The Weighted Linear Combination (WLC) method was used to integrate layers, resulting in a comprehensive suitability map of green spaces based on hierarchized criteria and their respective weights (dos Santos et al., 2021; Saeidi et al., 2017).

Step 5. The Zonal Land Suitability (ZLS) method: The ZLS method was employed to pinpoint areas with high suitability, considering a desirability threshold of 100, determined based on expert judgment, and a minimum site size requirement of one hectare (Eastman, 1999; Linh et al., 2022). In this method, which is a non-pixel, polygonal, and regional approach, there are three assumptions: 1) land use is always based on multiple objectives, 2) the best pixels from among the pixels of each map are identified for each use, and 3) the most preferred area for each use is selected. After preparing a macro file with the .iml extension, the Run Macro command was executed in the Trust software. Four main parameters are required to execute this command: the name of the input file, the desirability threshold (between 0 and 255), the minimum site size, and the name of the output file. The output consists of two tables and two maps. One of the tables provides statistical information about the area based on the station number, and the second table shows the area of suitable sites. Similarly, one of the maps displays the station number, while the other illustrates the suitability value of GS in the area on a pixel-by-pixel basis (Eastman, 1999).

2.3.4. Simulating urban growth scenarios

SLEUTH Model: SLEUTH, primarily designed for urban growth simulation, utilizes input data such as Slope, Land use, Exclusion, Urban extent, Transportation, and Hillshade (Yeh et al., 2021).

Simulating urban growth in SLEUTH often involves a weighted excluded layer, which serves to restrict or direct urban expansion in areas deemed unsuitable for development, such as protected lands or areas with high environmental value. By adjusting the excluded layer or modifying growth coefficients, urban development policies can be more accurately reflected, leading to more reliable simulation outcomes (Li et al., 2018a). SLEUTH includes four growth behaviors and is regulated by five coefficients (Li et al., 2018a; Rafiee et al., 2009; Salman Mahiny and Gholamalifard, 2006). SLEUTH comprises test, calibration, and prediction modules. The test module verifies model execution, while the calibration and prediction modules simulate past and forecast future urban changes (Salman Mahiny and Gholamalifard, 2006). The final calibration produces the Optimal SLEUTH Metric (OSM), used to rank coefficient combinations for the best fit, ensuring model accuracy (Dietzel and Clarke, 2006). The OSM assesses the accuracy of the model's growth quantity through the compare and pop parameters, while edges and clusters evaluate the size and shape of growth. The xmean and ymean account for the slope and spatial accuracy of the growth location. The range of OSM values varies between 0 and 1, with higher values indicating a better fit between simulated results and actual outcomes (J. Liu et al., 2017) (Eq. 2):

$$OSM = compare \times pop \times edges \times clusters \times slope \times xman \times yman \times Fmatch \quad (2)$$

Higher OSM values indicate a more accurate simulation, closely resembling real-world data. Utilizing the Monte Carlo iteration method and historical data, the model iteratively narrows control coefficient ranges to find optimal values, enabling accurate reproduction of past urban expansion and prediction of future changes. The SLEUTH model requires grid data, including slope and excluded layers, as well as urban, transportation, and hillshade layers. Roads were excluded from urban development as an excluded layer. The urban and transportation layers were obtained by extracting urban land use from the LULC map for the years 1989, 2001, 2013, and 2021. After calibrating and evaluating the model, predictions were made using the entire dataset and 150 Monte Carlo iterations, as recommended by the SLEUTH model guidelines by Mahiny and Clarke (2012) (A. S. Mahiny and Clarke, 2012).

Simulation Scenarios: After successfully calibrating the model, average values were used in prediction mode to simulate the future of Bojnourd City. SLEUTH offers a simulation platform for assessing the impact of policies implemented by decision-makers

Table 2
Selected factors for GS suitability.

Criteria	Sub-criteria	Sources/References
Climate	Temperature, evaporation	
Vegetation	NDVI, Range condition	(Li et al., 2018b; Ustaoglu and Aydinoglu, 2020)
Water		
sconces	Distance from river, spring, well and others	
Topography	Slope, aspect, elevation	
Land cover	Current LULC, distance from main/secondary roads, distance from residential areas, distance from reservoir, distance from historical sites, distance from pollution sources	(Gelan, 2021; Li et al., 2018b; Pokhrel, 2019; Sharma et al., 2022; E. Ustaoglu and Aydinoglu, 2020)
Geology	Erosion susceptibility	
	Geology	
Hazards	Landslide/Fire/ susceptibility	
	Earthquake-flood probabilities	(Anteneh et al., 2022; Gelan, 2021; Li et al., 2018b)

(Sakieh et al., 2015). There are three common methods to simulate various scenarios with SLEUTH. In the first method, different protection values are assigned to specified regions in the removed layer (A. Mahiny and Clarke, 2013; A. S. Mahiny and Clarke, 2012; Saeidi et al., 2018). In the second method, parameters influencing urban growth rules are adjusted to shape the form of urban expansion. Lastly, the third method involves manipulating self-organization constraints (Rafiee et al., 2009; Sakieh et al., 2015). In this study, the first method was applied using two excluded layers (MCE and CSS results), and the second method was implemented by adjusting the coefficients as proposed by Sakieh et al. (2015).

Operating the model necessitates the inclusion of one slope layer, two land use layers, one excluded layer, four urban layers, two transportation layers, and one hillshade layer as prerequisites. Slope constrains urban growth up to a critical level, while hillshade functions as a backdrop for displaying LULC predictions (Liu et al., 2020a).

Five scenarios were developed to simulate the growth of Bojnourd City over the next 29 years:

- 1- Historical Urban Growth (HUG): This scenario assumes that the city will continue to develop following its historical growth patterns, with no significant progress, improvements in green space, or changes in land use patterns. Calibrated coefficients are directly applied in the model's prediction mode, assuming the continuation of the current trend in urban growth.
- 2- Green City (GC): In this scenario, the urban growth pattern is restricted by the suitability of GS as indicated on a map. Expanding GS is prioritized to enhance the urban living environment and improve thermal comfort. Urban growth is limited based on environmental considerations, aiming to balance development with ecological preservation.

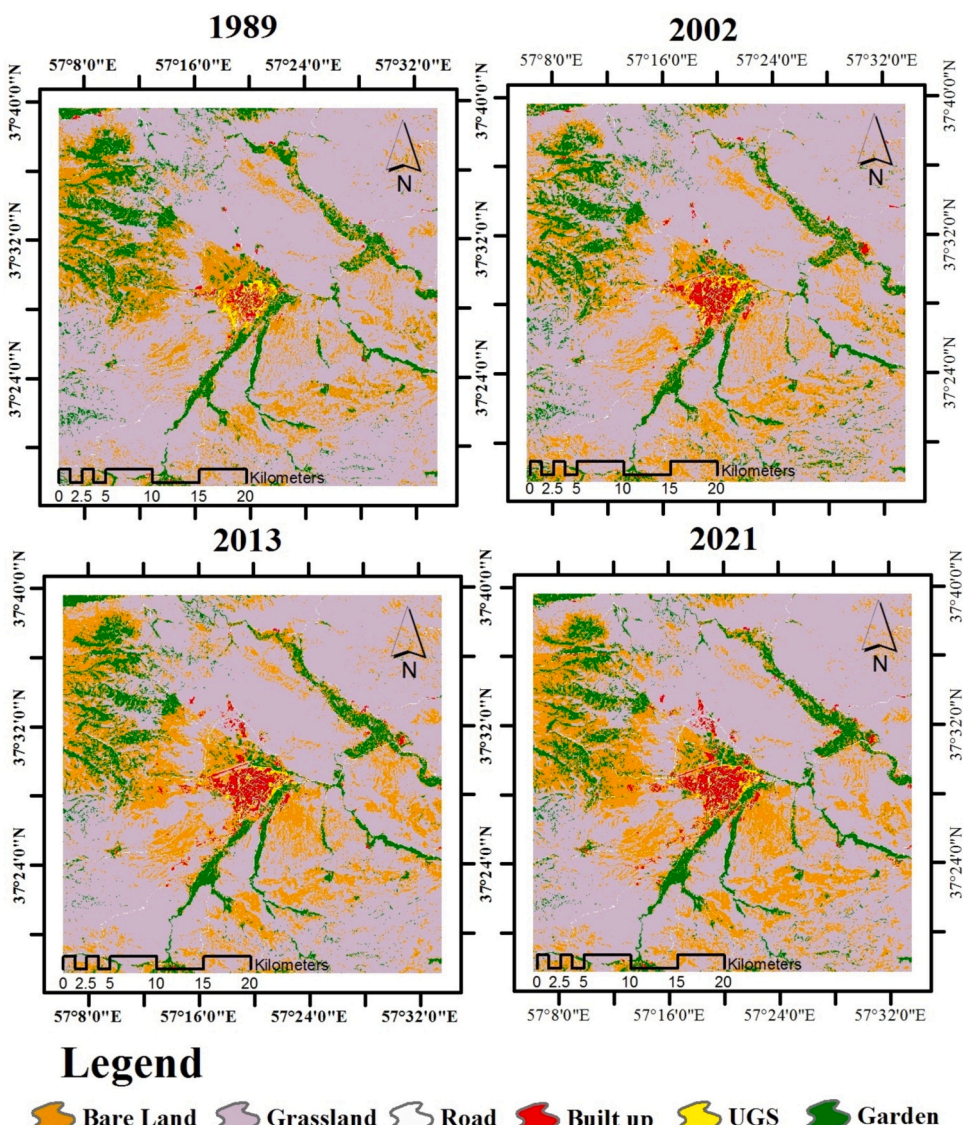


Fig. 3. LULC map from 1989 to 2021.

- 3- Low Carbon City (resilient) scenario (LCC): Urban growth in this scenario is constrained by the Carbon Sequestration Suitability (CSS) map. The aim is to limit carbon emissions and enhance resilience by directing development to areas suitable for carbon sequestration. This scenario emphasizes sustainable development practices to mitigate climate change impacts.
- 4- This scenario promotes urban growth near core cities to improve urban land connectivity and compactness. Spread and breed parameters are reduced from 38 and 35 to 15, respectively, to encourage infill urban development and protect the city's immediate environment from excessive urbanization. The goal is to create more sustainable and efficient urban areas.
- 5- Uncontrolled Urban Growth (UUG): This scenario represents uncontrolled and extensive forms of urban growth. Urban expansion is predicted to be substantial, with spread and breed coefficients increased from 38 and 35 to 55 each, respectively. The scenario reflects a lack of planning and regulation, resulting in rapid and often unsustainable urban sprawl.

2.3.5. Prioritizing scenarios by utilizing landscape metrics

Landscape Metrics analysis: Landscape metrics are crucial for providing a quantitative framework for assessing spatial and temporal characteristics within a landscape (Jia et al., 2019). Mean of patch area (AREA_MN), Number of Patches (NP), Patch Density (PD), Landscape Shape Index (LSI), Mean of Euclidean nearest-neighbor distance (ENN-MN), Perimeter-Area Fractal Dimension (PAFRAC), Mean fractal dimension index (FRAC-MN), and Mean shape index (SHAPE-MN) (Bakshi and Esraz-Ul-Zannat, 2023; Chakraborti et al., 2018; Cushman et al., 2008; Parvar et al., 2024a), were utilized to analyze simulated urban growth scenarios in 2050. These metrics were selected for their ability to capture the dynamics of the urban landscape and quantify newly generated patch information at the local level (Chakraborti et al., 2018).

Prioritization: In this study, the TOPSIS method was utilized to rank different scenarios. The calculations were implemented in the Python software package PYSIS with an easy interface developed by Salmanmahiny et al. (2022) (<https://mte.gau.ac.ir/NewsDetails?newsid=15497>).

The weights and desirability of each metric were determined based on expert insights. In this study, a team of seven experts in landscape ecology and environmental studies provided insights for determining the weights. To ensure simplicity and balance, all metrics were weighted equally at 0.125, under the assumption that each metric would have an equal influence on the outcomes. For landscape metrics, each one can either positively (MAX) or negatively (MIN) affect the built-up class. This prioritization can be adjusted based on expert perspectives. The sensitivity analysis involved randomly adjusting weights within a specified range, ensuring their total sum remained below 1 (Leonelli and Keane, 2012). This process was repeated 100,000 times, with weights changing by a maximum of 50 %.

3. Results

3.1. Change detection of LULC and LST

Six LULC types were identified (Fig. 3 and Table 3). The results, indicating overall accuracy rates of 92.59 %, 87.41 %, and 90.74 % for 2002, 2013 and 2021, along with Kappa coefficients of 0.91, 0.846, 0.887, and 0.864, respectively, which correctness and accuracy of the classification will be confirmed.

From 1989 to 2021, the built-up class has significantly increased, with a change rate of 178.94 %, while road and bare land classes have increased at rates to 37.86 % and 18.10 %, respectively. Conversely, garden, grassland, and UGS have experienced declines of 6.32 %, 6.46 %, and 38.90 %, highlighting the impact of human activities such as development, construction, and dry farming as predominant factors influencing the region's changes.

Mean seasonal daytime LST data across the study area from 1989 to 2021 were analyzed in the study. The LST data were obtained and processed to derive seasonal averages, encompassing winter, spring, summer, and autumn. The seasonal analysis revealed significant variations in daytime LST:

Winter: The LST ranged from -14.9°C to 13.4°C , marking the lowest temperatures observed.

Spring: LST values ranged from 11.7°C to 37.2°C .

Summer: The highest temperatures were recorded, with LST ranging from 36.3°C to 47.9°C .

Table 3
Area and percentages of LULC classes from 1989 to 2021.

Year	Unit	Road	Grassland	UGS*	Build up	Garden	Bare land
1989	Area (Km^2)	12.22	1117.47	5.30	10.75	160.14	334.36
	(%)	0.75	68.13	0.32	0.66	9.79	20.38
2002	Area (Km^2)	12.31	1100.67	4.49	20.90	159.54	342.34
	(%)	0.75	67.10	0.27	9.73	9.73	20.87
2013	Area (Km^2)	16.09	1070.69	3.04	25.90	147.45	337.08
	(%)	0.98	65.28	0.19	1.58	8.99	22.99
2021	Area (Km^2)	16.85	1045.24	3.23	30.00	150.02	394.91
	(%)	1.03	63.72	0.20	1.83	9.15	24.08
1989–2021	Changes (km^2)	4.63	-72.00	-2.06	19.24	-10.13	60.55
	Change rate (%)	37.86	-6.46	-38.90	178.94	-6.32	18.10

*Urban Green Space (UGS).

Autumn: LST ranged from 21.2 °C to 38 °C.

Additionally, an overall rising trend in mean annual LST was detected over the 32-year period, with an average increase rate of 0.018 °C per year (Fig. 4 A-B).

Seasonal variability in LST, with the highest temperatures consistently occurring in summer and the lowest in winter. The observed long-term trend suggests a gradual warming of the study area, which may be attributed to various climatic and anthropogenic factors.

The relative contribution of each LULC class to LST during the summers of 1989, 2002, 2013, and 2021 was investigated, in addition to examining seasonal changes (Fig. 4C). It was observed that the mean LST for nearly all classes, with the exception of UGS, has been found to increase over the study period. Barren land and rangeland were identified as having the highest share in the creation of hot spots.

3.2. CSS mapping

The difference in carbon stored (Mg of C) per pixel between current and future (the next considered year) landscape is shown in Fig. 5. Negative values indicate lost carbon and positive values with light color indicate carbon sequestration. During the period of urbanization development from 1989 to 2021, there was a decrease in the total carbon stocks by $-101,974.20$ (Mg of C).

3.3. GS suitability assessment

The seven main criteria used to prepare the GS suitability map were selected based on previous studies (Li et al., 2018b; Linh et al., 2022; E Ustaoglu, 2022; Ustaoglu and Aydinoglu, 2020). Vegetation received the highest weight (0.3375), while geology was given the lowest (0.0379); climate (0.0536), land cover (0.2160), topography (0.0834), and both water sources and hazards (each 0.1358) were weighted accordingly. The consistency ratio (CR) was 0.01, indicating a high level of consistency. These weights, assigned by a panel of 15 experts, were applied to generate the final suitability map through a weighted overlay of the selected layers.

High-suitability regions for GS in Bojnourd City include existing green areas and northern sectors dominated by agriculture, particularly gardens, covering 17,300 ha. Moderately suitable areas, totaling 34,550 ha, are found around the city, mainly in the southern and western regions, where agricultural land is distanced from residential areas. Lower-suitability regions, scattered throughout the study area, account for 16,950 ha.

In light of these criteria, new filters were applied to the suitability map, and the highly suitable pixels were incorporated as an excluded layer in SLEUTH urban growth modeling (Fig. 6).

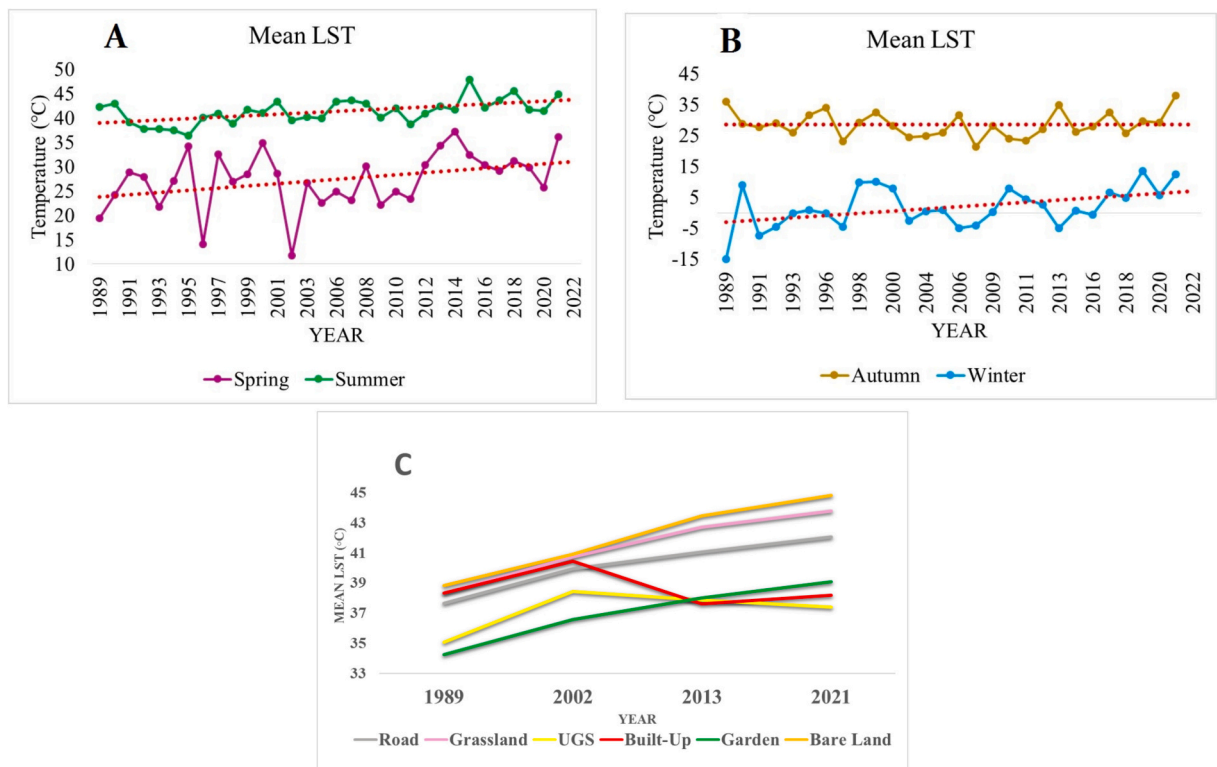


Fig. 4. Temporal evolution of seasonal mean LST trends during spring and summer (A) and autumn and winter (B) from 1989 to 2021. Relative contribution of each LULC class on LST for the years 1989, 2002, 2013, and 2021 (C).

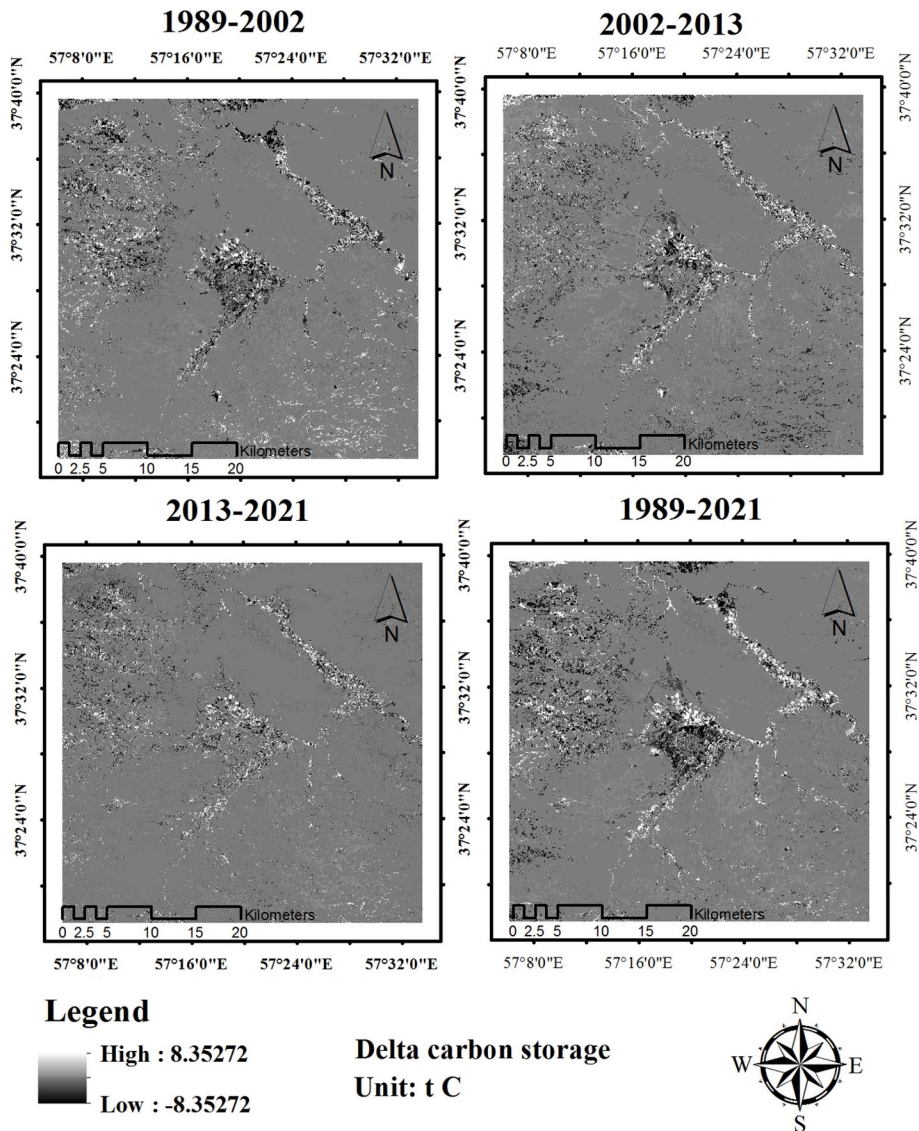


Fig. 5. Carbon storage from 1989 to 2021.

3.4. SLEUTH model

3.4.1. Model calibration

The initial SLEUTH model underwent coarse, fine, and final calibration based on historical data from the study area. OSM determined the best fit at each calibration stage, sorting coefficients to gradually narrow the control coefficient range until identifying the best growth control coefficients. A summary of the Model calibration is presented in Table 4.

As indicated in Table 4, slope resistance and road gravity have a more significant influence on city growth, while diffusion, spread, and breed play a comparatively lesser role.

3.4.2. Simulation of urban growth

Fig. 7 presents the results of simulating urban growth scenarios up to 2050 under five scenarios. The predicted historical trend implies a probability of urban expansion of approximately 5496.3 ha of land by the year 2050. Across scenarios, LCC represents 5073.1 ha, CUG represents the lowest growth at 2938.6 ha, UUG represents the highest growth at 8693.1 ha, and GC represents an intermediate expansion of 4476.4 ha.

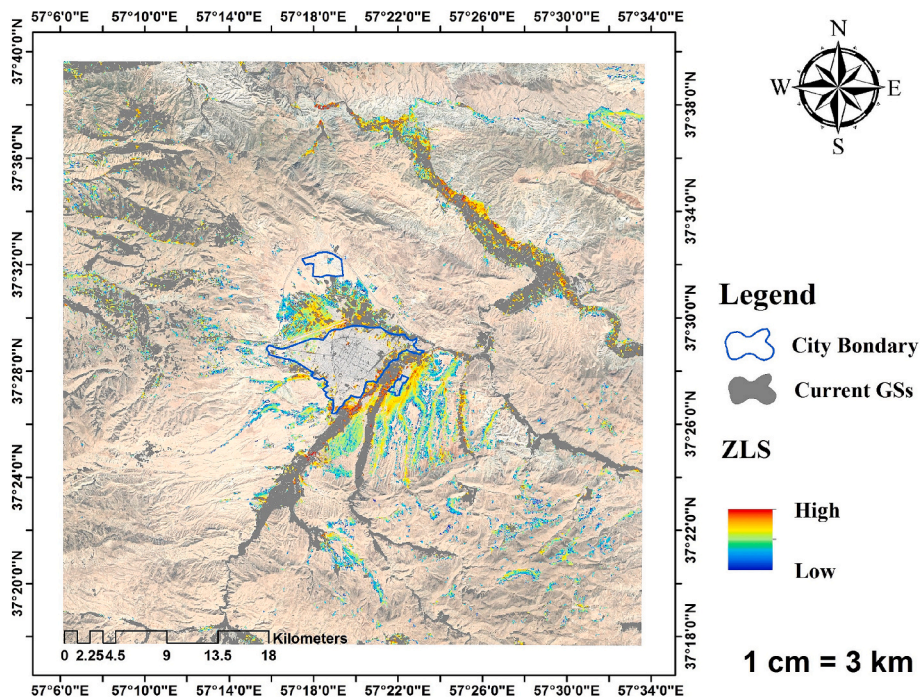


Fig. 6. Green space suitability map. (For interpretation of the references to color in this figure legend, the reader is referred to the web version of this article.)

Table 4
Summary of model calibration process and coefficients.

GC	Coarse		Fine		Final		BFC
	MCI = 4	NI = 3125	MCI = 8	NI = 12,348	MCI = 10	NI = 4096	
	Start-End	Step	Start-End	Step	Start-End	Step	
Diffusion	0–100	25	20–30	2	18–24	2	30
Breed	0–100	25	20–40	3	22–28	2	35
Road gravity	0–100	25	20–30	2	24–30	2	49
Slope	0–100	25	80–100	3	96–99	1	92
Spread	0–100	25	20–80	10	40–80	4	38

GC: Growth Coefficients BFC: Best Fit Coefficient - MCI: Monte Carlo Iterations -Number of Iterations

3.5. Landscape metrics analysis and TOPSIS prioritization

Landscape metrics were extracted to assess and compare different urban growth scenarios (Table 5). These metrics provide insights into the diverse patterns and impacts associated with each scenario.

The prioritization of urban growth scenarios, employing landscape metrics alongside the TOPSIS method, is detailed in Fig. 8 and Table 6. All metrics were weighted equally at 0.125.

Based on the results of TOPSIS using landscape metrics values, the CUG scenario, which prioritizes land conservation, achieved the highest environmental sustainability score of 0.818. It was followed by the GC scenario with a score of 0.72, and the LCC scenario with a score of 0.55. To ensure the robustness of the TOPSIS results, sensitivity testing was conducted by introducing a maximum variation of 50 % in the weights of the profiles, involving 100,000 iterations. All iterations yielded consistent outcomes with the initial rankings.

4. Discussion

4.1. LULC and LST changes

LULC changes play a significant role in the increase of LST. In the study area, urban areas exhibit lower LST compared to the

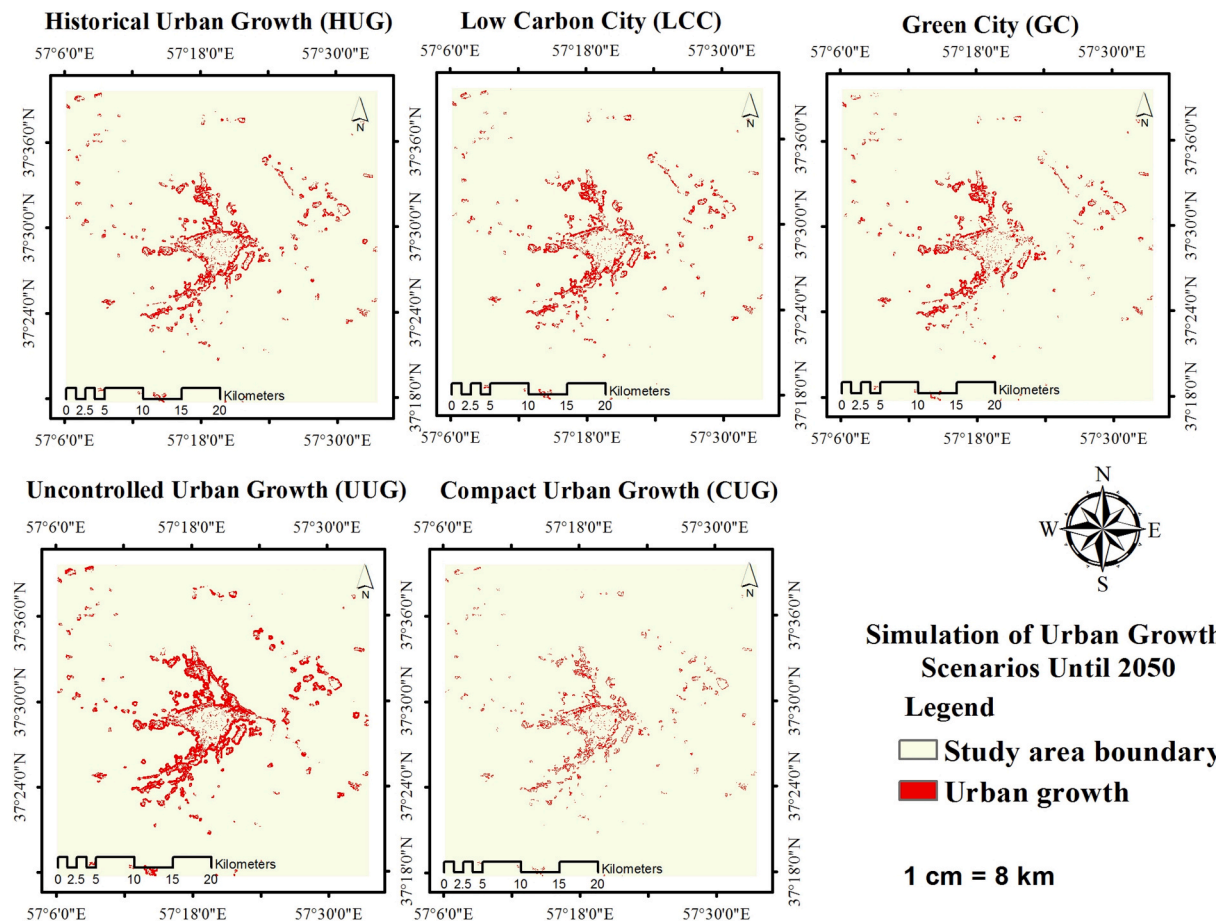


Fig. 7. Simulation of urban growth scenarios until 2050.

Table 5

Comparison of different urban growth scenarios using landscape metrics.

Desirability	Max	Max	Max	Min	Max	Max	Min	Max
Weights	0.125	0.125	0.125	0.125	0.125	0.125	0.125	0.125
Metrics	NP	PD	LSI	AREA_MN	PAFRAC	FRAC_MN	ENN_MN	SHAPE_MN
LCC	328	0.2	27.39	28.36	1.28	1.06	292.7	1.56
CUG	402	0.24	23.48	17.83	1.23	1.04	236.7	1.32
Scenarios	HUG	287	0.17	22.76	33.89	1.23	1.05	325.4
	UUG	295	0.18	23.81	47.81	1.23	1.05	352.4
	GC	367	0.22	26.24	23.72	1.27	1.06	298.2

Max: Positive effect of metrics/Min: Negative effect of metrics.

Number of Patches (NP), Patch Density (PD), Landscape Shape Index (LSI), Mean of patch area (AREA_MN), Perimeter-Area Fractal Dimension (PAFRAC), Mean fractal dimension index (FRAC-MN), Mean of Euclidean nearest-neighbor distance (ENN-MN), and Mean shape index (SHAPE-MN).

surrounding lands. This disparity is primarily due to the surrounding semi-arid environment, characterized by prevalent bare and sandy grounds, which absorb and retain more heat (Parvar et al., 2024a). In such semi-arid regions, the role of green spaces becomes even more critical, highlighting the necessity for strategic urban development policies. According to Ouma et al. (2021), the elevated LST in barren land is attributed to dry sandy soils, which exhibit properties somewhat similar to constructed concrete or asphalted surfaces (Ouma et al., 2021). Over the past 32 years, the study area has experienced significant changes in LULC, with a particularly remarkable 178 % increase in built-up areas. Furthermore, an analysis of seasonal mean LST trends within the study area, conducted under cloudless conditions, has revealed a gradual increase over time. This observed trend suggests an annual rate of LST change of approximately 0.2 % (based solely on Landsat images acquired on days with minimal cloud cover, representing the average across these days). Such findings underscore the local manifestation of global temperature trends and highlight the urgent need for proactive measures to address the impacts of climate change.

Global trends show a notable increase in LST between 2001 and 2017, supported by various studies (Liu et al., 2020b; Rani and Mal,

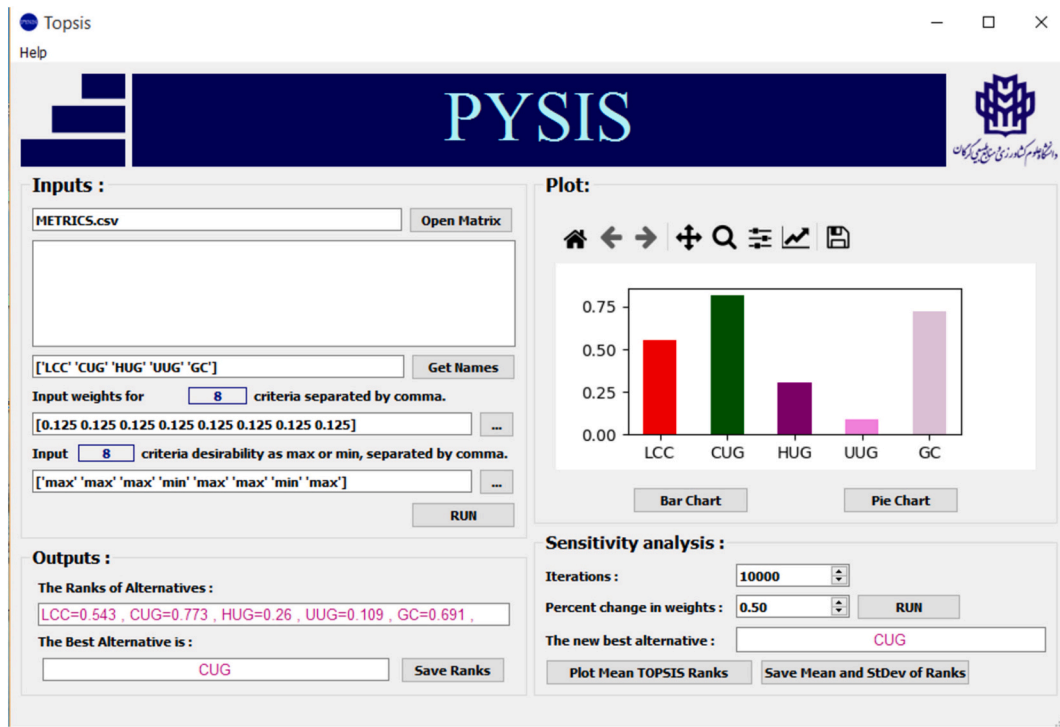


Fig. 8. The prioritization of urban growth scenarios in PYYSIS software (Ref: <https://mte.gau.ac.ir/NewsDetails?newsid=15497>).

Table 6

The priority of urban growth scenarios based on landscape metrics using the TOPSIS method.

Rank	1	2	3	4	5
Scenarios	GC	CUG	LCC	HUG	UUG
The rank of alternatives	0.72	0.818	0.555	0.303	0.092
Ranks with sensitivity analysis	0.691	0.773	0.543	0.26	0.109

The score ranges vary between 0 and 1, where a higher score denotes better environmental sustainability.

2022; Song et al., 2018). Rani and Mal (2022) highlighted a significant rise in mean daytime LST across High Mountain Asia, observable on both seasonal and annual scales. This warming trend, while indicative of broader climate changes, also reflects changes in LULC affecting regional temperature dynamics.

4.2. Landscape patterns

Landscape metrics offer quantitative evaluation of landscape patterns, aiding planners in prioritizing urban development scenarios. In this study, utilizing landscape metrics, the preferred scenarios were chosen, enabling informed decision-making. This approach not only supports the creation of sustainable urban environments but also enhances resilience to climate challenges, ultimately benefiting urban residents' well-being.

Each landscape criterion may have a positive or negative impact, depending on the city managers' preferred development approach, as explained below:

Higher values of NP indicate a greater allocation of GS among urban blocks, thus eliciting a positive effect. Considering this, the CUG, LCC, and GC scenarios are considered the most favorable. However, NP is not the only metric that planners should consider.

Another crucial metric is PD, the significance of which varies depending on the nature of urban development and the availability of spaces for future city growth. If planners prioritize land conservation, then high PD values may be desirable, as seen in scenarios like CUG and GC.

A high LSI value in urban patches indicates a high degree of complexity in their configuration (McGarigal, 2015). From this perspective, scenarios such as LCC and GC are considered preferable, respectively. The interpretation of the AREA-MIN metric can vary based on the specific objectives of urban development. High values of AREA-MIN might be considered unfavorable if they indicate excessive allocation of land to urban use, but they could be viewed as favorable if they align with the objectives of urban development. The UUG and HUG scenarios showed the highest values and cannot be preferred scenarios.

A decrease in the nearest neighbor distance suggests that urban patches are more aggregated (McGarigal, 2015). Conversely, an increase in the distance between neighboring patches leads to greater isolation of these patches. ENN_MN was considered as a metric with a negative impact on the selection of the urban growth scenario.

Shape metrics such as PAFRAC, FRAC-MN, and SHAPE-MN were also analyzed as indicators with a positive impact. The complexity of the shape of urban areas demonstrates that urban growth has not disregarded ecologically valuable lands.

Quantifying various aspects such as patch distribution, size, and connectivity, landscape metrics furnish invaluable insights into the dynamic urban landscape and its profound implications for resource management and environmental sustainability (Asgarian et al., 2015; Bakshi and Esraz-Ul-Zannat, 2023; Madanian et al., 2018).

Despite the valuable insights offered by landscape metrics, there remains a significant lack of research focusing on their practical and operational implementation within urban planning.

Notably, research has underscored the pivotal role of landscape arrangement in mitigating urban heat, thus contributing to the cooling of urban environments (Asgarian et al., 2015; Effati et al., 2021; Osborne and Alvares-Sanches, 2019).

Some previous studies have concentrated on employing metrics to delineate urban boundaries (Sun and Shao, 2020; Unal Cilek and Cilek, 2021). A notable endeavor by Bakshi and Esraz-Ul-Zannat (2023) employed landscape metrics to scrutinize urban patch characteristics, including pattern, size, and aggregation, based on simulated urban maps.

4.3. Urban growth scenarios

Analyzing urban growth scenarios identifies impacts on land use and sustainability, informing decisions for balanced development.

HUG scenario forecasts a notable urban expansion to 9727 ha by 2050, in line with present growth trends, forming separate patches in its north and south. This fragmented growth poses risks of urban landscape fragmentation and requires additional human development, altering surrounding land use. Urban growth projections rely on past data, assuming consistency in land-use policies and development decisions. However, as noted by Varquez et al. (2023), real-world events and urban planning strategies can alter future pathways and human mobility (Varquez et al., 2023). Because there are garden and cultural lands near the city's edges, it's important to realize that the current trend of urban growth can't continue.

The UUG scenario forecasts a 12,924.4-ha expansion, emphasizing the risk of uncontrolled development on valuable peri-urban and available vacant land within the city. As Sakieh et al. (2015) pointed out in their study in Karaj, the current formation of separated urban patches should not encourage smaller clusters to expand outward. Instead, they recommend that each urban cluster initiates its growth cycle, particularly in areas with available vacant land within the internal urban environment (Sakieh et al., 2015).

According to the landscape metrics analysis, the CUG scenario was selected as the preferred scenario for urban development. This scenario is pivotal in preserving valuable lands and minimizing the conversion of agricultural fields into impermeable surfaces. It achieves this by maintaining green spaces in peri-urban areas and preserving green belts and ecological corridors. The CUG approach enhances the efficient use of land resources, fostering resilience and sustainability in urban environments.

The GC scenario emerged as the next preferred option, integrating a green suitability decision rule to accurately depict preserved parks and potential GS areas. This model ensures sufficient allocation of space within city blocks for greenery, thus enhancing urban environmental quality. This finding aligns with Saxena and Jat (2019) research, where they incorporated a suitability map of urban development into their model, resulting in enhanced depiction of small-scale, fragmented, and roadside developments. Their study emphasized the superiority of modeling based on suitability maps over the original model.

The LCC scenario targets preserving urban and peri-urban ecosystem services, particularly carbon storage, amid extensive impervious surfaces in urban areas. Given the significant contribution of the built environment to global greenhouse gas emissions, promoting GS expansion and enhancing urban landscapes' aesthetics are encouraged to improve citizens' well-being and sustainable urban living. The carbon stock and sequestration model helps design scenarios to meet greenhouse gas reduction targets effectively (Chuai et al., 2014; Jiang et al., 2017). Some studies have highlighted the significance of integrating carbon models into urban growth or land use change scenarios (Jiang et al., 2017; Mohammadyari et al., 2023; Zarandian et al., 2023). Mohammadyari et al. (2023) suggested that employing ecosystem services to optimize LULC allocation is valuable. This strategy allows consideration of both ecosystem function and structure in planning decisions, aiding land managers in developing sustainable LULC plans that maintain ecosystem services.

Hwang et al. (2022), employed a simulation model to investigate the impact of land use changes on carbon storage. They concluded that creating green belts, designated areas of undeveloped land, could serve as effective carbon storage reservoirs. This approach not only safeguards future carbon storage but also helps mitigate urban sprawl, promoting the preservation of natural habitats and preventing excessive urban expansion.

The study's preferred scenario, Scenario CUG, emphasizes land conservation as a policy objective. In the broader context of urban planning, the discourse surrounding land-sharing and land-sparing strategies delves deep into the intricate mechanisms of optimizing ecosystem services crucial for the sustainable development of cities. As highlighted by Osborne and Alvares-Sanches (2019), this discussion underscores the paramount importance of factors such as temperature regulation, which is intricately linked to the presence and management of green spaces within urban environments (Osborne and Alvares-Sanches, 2019). Land-sharing proponents advocate for a model where low-density built areas coexist harmoniously with ample greenery dispersed throughout the urban landscape (GS and LCC scenarios). On the other hand, proponents of the land-sparing strategy prioritize the concentration of development into high-density built environments while preserving larger, contiguous expanses of green spaces on the city's outskirts or within designated areas (CUG scenarios). This approach ensures that urban growth does not encroach excessively on natural habitats, preserving crucial ecosystems and biodiversity hotspots.

Both approaches have their merits and challenges, and the choice between land-sharing and land-sparing strategies often depends on various factors such as urban density, available land, socio-economic considerations, and environmental objectives. Ultimately, successful urban planning requires a nuanced understanding of these strategies and their implications to create cities that are not only functional and efficient but also sustainable and resilient in the face of environmental challenges.

4.4. Limitations and recommendations

This study employed a GS suitability map as a constraint in urban development. While such maps are useful in urban planning, their creation involves inherent limitations. Policymakers should exercise caution due to cities' dynamic nature and the constraints of using static data and modeling techniques. Careful consideration is necessary, taking into account the evolving urban environment. The study suggests optimizing land uses for sustainable urban development. Future research should explore integrating modeling and optimization techniques to achieve optimal land use patterns, addressing challenges in balancing urban development priorities effectively.

5. Conclusions

In Bojnourd City's dynamic landscape, significant shifts in both LULC and LST have occurred from 1989 to 2021, largely due to rapid urbanization and infrastructure expansion. This study contributes to informed decision-making for climate-resilient urban management by presenting and analyzing various scenarios. Key findings from this research are:

Landscape metrics offer valuable quantitative insights into the desirability of various urban growth scenarios and reflect diverse urban planning policies. These metrics help urban planners assess the effectiveness of different policies and strategies, providing a comprehensive understanding of the implications of each scenario. This connection between metrics and policy effectiveness enables decision-makers to prioritize initiatives that align with sustainable and resilient urban development goals.

The CUG scenario focuses on land conservation, while the GS and LCC scenarios include broader strategies, such as expanding green spaces and enhancing urban green ecosystem services. These multifaceted approaches highlight the integration of GS expansion with sustainable urban planning, significantly enhancing urban sustainability and resilience against climate change challenges.

The study emphasizes the importance of increasing urban green spaces and implementing rational land use policies to reduce carbon losses and achieve a balanced carbon footprint. It stresses the need to prioritize the protection of ecological and cultivated land to prevent fragmentation and preserve valuable ecosystems. This integrated approach connects GS enhancement with sustainable land use planning, promoting long-term environmental sustainability.

The proposed approach offers crucial insights for planners and decision-makers to evaluate the impacts of current urban spatial planning policies on future urban growth. The connection between landscape metrics, scenario analysis, and GS policies provides a unified framework for promoting sustainable and resilient urban development.

CRediT authorship contribution statement

Zahra Parvar: Writing – review & editing, Writing – original draft, Visualization, Validation, Software, Methodology, Conceptualization, Formal analysis, Investigation. **Marjan Mohammadzadeh:** Writing – review & editing, Supervision, Conceptualization. **Sepideh Saeidi:** Writing – review & editing, Supervision, Conceptualization.

Declaration of competing interest

The authors declare that they have no known competing financial interests or personal relationships that could have appeared to influence the work reported in this paper.

Data availability

No data was used for the research described in the article.

Acknowledgment

This research is based on the first author's PhD dissertation. In addition to the guidance provided by the supervisory team at Gorgan University of Agricultural Sciences and Natural Resources, we would like to sincerely thank Professor Abdolrasoul Salmanmahiny for his invaluable guidance and constructive feedback, which significantly improved the overall quality of this research.

References

Aburas, M.M., Ho, Y.M., Ramlı, M.F., Ash'aari, Z.H., 2017. Improving the capability of an integrated CA-Markov model to simulate spatio-temporal urban growth trends using an analytical hierarchy process and frequency ratio. *Int. J. Appl. Earth Obs. Geoinf.* 59, 65–78.

Adelisardou, F., Zhao, W., Chow, R., Mederly, P., Minkina, T., Schou, J.S., 2022. Spatiotemporal change detection of carbon storage and sequestration in an arid ecosystem by integrating Google earth engine and InVEST (the Jiroft plain, Iran). *Int. J. Environ. Sci. Technol.* 19 (7), 5929–5944. <https://doi.org/10.1007/s13762-021-03676-6>.

Ahmadi Mirghaed, F., Mohammadzadeh, M., Salmanmahiny, A., Mirkarimi, S.H., 2020. Decision scenarios using ecosystem services for land allocation optimization across Gharehsoo watershed in northern Iran. *Ecol. Indic.* 117, 106645. <https://doi.org/10.1016/j.ecolind.2020.106645>.

Alavipanah, S., Schreyer, J., Haase, D., Lakes, T., Qureshi, S., 2018. The effect of multi-dimensional indicators on urban thermal conditions. *J. Clean. Prod.* 177, 115–123. <https://doi.org/10.1016/j.jclepro.2017.12.187>.

Anteneh, M.B., Damte, D.S., Abate, S.G., Gedefaw, A.A., 2022. A Geospatial Assessment of Urban Green Space in Debre Markos City, Ethiopia.

Ariluoma, M., Ottelin, J., Hautamäki, R., Tuukkanen, E.-M., Mänttäri, M., 2021. Carbon sequestration and storage potential of urban green in residential yards: A case study from Helsinki. *Urban For. Urban Green.* 57, 126939. <https://doi.org/10.1016/j.ufug.2020.126939>.

Asgarian, A., Amiri, B.J., Sakieh, Y., 2015. Assessing the effect of green cover spatial patterns on urban land surface temperature using landscape metrics approach. *Urban Ecosyst.* 18 (1), 209–222. <https://doi.org/10.1007/s11252-014-0387-7>.

Azmi, R., Tekouabou Koumetou, C.S., Diop, E.B., Chenal, J., 2021. Exploring the relationship between urban form and land surface temperature (LST) in a semi-arid region case study of Ben Guerir city - Morocco. *Environ. Challenges* 5, 100229. <https://doi.org/10.1016/j.envc.2021.100229>.

Bai, T., Mayer, A.L., Shuster, W.D., Tian, G., 2018. The hydrologic role of urban green space in mitigating flooding (Luohu, China). *Sustainability* 10 (10).

Bakshi, A., Esrafil-Zannat, M., 2023. Application of urban growth boundary delineation based on a neural network approach and landscape metrics for Khulna City, Bangladesh. *Helijon* 9 (6), e16272. <https://doi.org/10.1016/j.helijon.2023.e16272>.

Cao, Y., Carver, S., Yang, R., 2019. Mapping wilderness in China: comparing and integrating Boolean and WLC approaches. *Landsc. Urban Plan.* 192, 103636. <https://doi.org/10.1016/j.landurbplan.2019.103636>.

Chakraborti, S., Das, D.N., Mondal, B., Shafizadeh-Moghadam, H., Feng, Y., 2018. A neural network and landscape metrics to propose a flexible urban growth boundary: a case study. *Ecol. Indic.* 93, 952–965.

Change, I., 2006. 2006 IPCC Guidelines for National Greenhouse Gas Inventories. Institute for Global Environmental Strategies, Hayama, Kanagawa, Japan.

Chaudhuri, G., Clarke, K.C., 2019. Modeling an Indian megalopolis- A case study on adapting SLEUTH urban growth model. *Comput. Environ. Urban. Syst.* 77, 101358. <https://doi.org/10.1016/j.compenvurbsys.2019.101358>.

Cheng, Y., Farmer, J.R., Dickinson, S.L., Robeson, S.M., Fischer, B.C., Reynolds, H.L., 2021. Climate change impacts and urban green space adaptation efforts: evidence from U.S. municipal parks and recreation departments. *Urban Clim.* 39, 100962. <https://doi.org/10.1016/j.uclim.2021.100962>.

Chuai, X., Huang, X., Wang, W., Wu, C., Zhao, R., 2014. Spatial simulation of land use based on terrestrial ecosystem carbon storage in coastal Jiangsu, China. *Sci. Rep.* 4 (1), 5667.

Cushman, S., McGarigal, K., Neel, M., 2008. Parsimony in landscape metrics: strength, universality, and consistency. *Ecol. Indic.* 8, 691–703. <https://doi.org/10.1016/j.ecolind.2007.12.002>.

Dietzel, C., Clarke, K., 2006. The effect of disaggregating land use categories in cellular automata during model calibration and forecasting. *Comput. Environ. Urban. Syst.* 30, 78–101. <https://doi.org/10.1016/j.compenvurbsys.2005.04.001>.

dos Santos, A.R., Anjinho, P.D.S., Neves, G.L., Barbosa, M.A.G.A., de Assis, L.C., Mauad, F.F., 2021. Dynamics of environmental conservation: evaluating the past for a sustainable future. *Int. J. Appl. Earth Obs. Geoinf.* 102, 102452. <https://doi.org/10.1016/j.jag.2021.102452>.

Eastman, J.R., 1999. Multi-criteria evaluation and GIS. *Geogr. Inf. Syst.* 1 (1), 493–502.

Effati, F., Karimi, H., Yavari, A., 2021. Investigating effects of land use and land cover patterns on land surface temperature using landscape metrics in the city of Tehran, Iran. *Arab. J. Geosci.* 14 (13), 1240. <https://doi.org/10.1007/s12517-021-07433-4>.

Eggleson, H., Buendia, L., Miwa, K., Ngara, T., Tanabe, K., 2006. 2006 IPCC Guidelines for National Greenhouse Gas Inventories.

Esmaelpour-Poodeh, S., Ghorbani, R., Hosseini, S.A., Salmanmahiny, A., Rezaei, H., Kamayab, H., 2019. A multi-criteria evaluation method for sturgeon farming site selection in the southern coasts of the Caspian Sea. *Aquaculture* 513, 734416. <https://doi.org/10.1016/j.aquaculture.2019.734416>.

Falah, N., Karimi, A., Harandi, A.T., 2020. Urban growth modeling using cellular automata model and AHP (case study: Qazvin city). *Model. Earth Syst. Environ.* 6 (1), 235–248. <https://doi.org/10.1007/s40808-019-00674-z>.

Feng, H.-H., Liu, H.-P., Lü, Y., 2012. Scenario prediction and analysis of urban growth using SLEUTH model. *Pedosphere* 22 (2), 206–216. [https://doi.org/10.1016/S1002-0160\(12\)60007-1](https://doi.org/10.1016/S1002-0160(12)60007-1).

Fusaro, L., Salvatori, E., Mereu, S., Marando, F., Scassellati, E., Abbate, G., Manes, F., 2015. Urban and peri-urban forests in the metropolitan area of Rome: ecophysiological response of Quercus ilex L. in two green infrastructures in an ecosystem services perspective. *Urban For. Urban Green.* 14 (4), 1147–1156. <https://doi.org/10.1016/j.ufug.2015.10.013>.

Gelan, E., 2021. GIS-based multi-criteria analysis for sustainable urban green spaces planning in emerging towns of Ethiopia: the case of Sululta town. *Environ. Syst. Res.* 10. <https://doi.org/10.1186/s40068-021-00220-w>.

Gounaris, D., Chorianopoulos, I., Symeonakis, E., Koukoulas, S., 2019. A random Forest-cellular automata modelling approach to explore future land use/cover change in Attica (Greece), under different socio-economic realities and scales. *Sci. Total Environ.* 646, 320–335.

Han, D., An, H., Wang, F., Xu, X., Qiao, Z., Wang, M., Sui, X., Liang, S., Hou, X., Cai, H., Liu, Y., 2022. Understanding seasonal contributions of urban morphology to thermal environment based on boosted regression tree approach. *Build. Environ.* 226, 109770. <https://doi.org/10.1016/j.buildenv.2022.109770>.

Han, D., An, H., Cai, H., Wang, F., Xu, X., Qiao, Z., Jia, K., Sun, Z., An, Y., 2023. How do 2D/3D urban landscapes impact diurnal land surface temperature: insights from block scale and machine learning algorithms. *Sustain. Cities Soc.* 99, 104933. <https://doi.org/10.1016/j.scs.2023.104933>.

Hwang, J., Choi, Y., Sung, H.C., Yoo, Y.-J., Lim, N.O., Kim, Y., Shin, Y., Jeong, D., Sun, Z., Jeon, S.W., 2022. Evaluation of the function of suppressing changes in land use and carbon storage in green belts. *Resour. Conserv. Recycl.* 187, 106600. <https://doi.org/10.1016/j.resconrec.2022.106600>.

Imen, G., Halima, G., Djamel, A., 2022. Relationship Between LULC Characteristic and LST Using Remote Sensing and GIS, Case Study GUELMA (Algeria).

Jafari, M., Majedi, H., Monavari, S.M., Alesheikh, A.A., Kheirkhah Zarkesh, M., 2016. Dynamic simulation of urban expansion based on cellular automata and logistic regression model: case study of the Hyrcanian region of Iran. *Sustainability* 8 (8), 810.

Jia, Y., Tang, L., Xu, M., Yang, X., 2019. Landscape pattern indices for evaluating urban spatial morphology – A case study of Chinese cities. *Ecol. Indic.* 99, 27–37. <https://doi.org/10.1016/j.ecolind.2018.12.007>.

Jiang, W., Deng, Y., Tang, Z., Lei, X., Chen, Z., 2017. Modelling the potential impacts of urban ecosystem changes on carbon storage under different scenarios by linking the CLUE-S and the InVEST models. *Ecol. Model.* 345, 30–40. <https://doi.org/10.1016/j.ecolmodel.2016.12.002>.

Kafy, A.A., Saha, M., Fattah, M.A., Rahaman, M.T., Dutti, B.M., Rahaman, Z.A., Bakshi, A., Kalaivani, S., Nafiz Rahaman, S., Sattar, G.S., 2023. Integrating forest cover change and carbon storage dynamics: leveraging Google earth engine and InVEST model to inform conservation in hilly regions. *Ecol. Indic.* 152, 110374. <https://doi.org/10.1016/j.ecolind.2023.110374>.

Kazemi, F., Hosseinpour, N., 2022. GIS-based land-use suitability analysis for urban agriculture development based on pollution distributions. *Land Use Policy* 123, 106426. <https://doi.org/10.1016/j.landusepol.2022.106426>.

Kumar, M., 2018. Landscape metrics for assessment of land cover change and fragmentation of a heterogeneous watershed. *Rem. Sens. App.* 10, 224–233. <https://doi.org/10.1016/j.rsase.2018.04.002>.

Leonelli, R.C.B., Keane, J.T., 2012. Enhancing a Decision Support Tool with Sensitivity Analysis.

Li, F., Wang, L., Chen, Z., Clarke, K.C., Li, M., Jiang, P., 2018a. Extending the SLEUTH model to integrate habitat quality into urban growth simulation. *J. Environ. Manag.* 217, 486–498. <https://doi.org/10.1016/j.jenvman.2018.03.109>.

Li, Z., Fan, Z., Shen, S., 2018b. Urban green space suitability evaluation based on the AHP-CV combined weight method: a case study of Fuping County, China. *Sustainability* 10 (8). <https://doi.org/10.3390/su10082656>.

Li, L., Song, Y., Wei, X., Dong, J., 2020. Exploring the impacts of urban growth on carbon storage under integrated spatial regulation: a case study of Wuhan, China. *Ecol. Indic.* 111, 106064. <https://doi.org/10.1016/j.ecolind.2020.106064>.

Liang, X., Liu, X., Li, D., Zhao, H., Chen, G., 2018. Urban growth simulation by incorporating planning policies into a CA-based future land-use simulation model. *Int. J. Geogr. Inf. Sci.* 32 (11), 2294–2316.

Linh, N.H., Tung, P.G., Chuong, H.V., Ngoc, N.B., Phuong, T.T., 2022. The application of geographical information systems and the analytic hierarchy process in selecting sustainable areas for urban green spaces: A case study in Hue City, Vietnam. *Climate* 10 (6).

Liu, J., Zhang, G., Zhuang, Z., Cheng, Q., Gao, Y., Chen, T., Huang, Q., Xu, L., Chen, D., 2017. A new perspective for urban development boundary delineation based on SLEUTH-InVEST model. *Habitat Int.* 70, 13–23. <https://doi.org/10.1016/j.habitatint.2017.09.009>.

Liu, D., Clarke, K.C., Chen, N., 2020a. Integrating spatial nonstationarity into SLEUTH for urban growth modeling: a case study in the Wuhan metropolitan area. *Comput. Environ. Urban. Syst.* 84, 101545. <https://doi.org/10.1016/j.compenvurbsys.2020.101545>.

Liu, J., Hagan, D.F.T., Liu, Y., 2020b. Global land surface temperature change (2003–2017) and its relationship with climate drivers: AIRS, MODIS, and ERA5-land based analysis. *Remote Sens.* 13 (1), 44.

Liu, X., Xu, H., Zhang, M., 2024. The effects of urban expansion on carbon emissions: based on the spatial interaction and transmission mechanism. *J. Clean. Prod.* 434, 140019. <https://doi.org/10.1016/j.jclepro.2023.140019>.

Madanian, M., Soffianian, A.R., Koupai, S.S., Pourmanafi, S., Momeni, M., 2018. Analyzing the effects of urban expansion on land surface temperature patterns by landscape metrics: a case study of Isfahan city, Iran. *Environ. Monit. Assess.* 190 (4), 189. <https://doi.org/10.1007/s10661-018-6564-z>.

Mahiny, A.S., Clarke, K.C., 2012. Guiding SLEUTH land-use/land-cover Change modeling using multicriteria evaluation: towards dynamic sustainable land-use planning. *Environ. Plan. B* 39 (5), 925–944. <https://doi.org/10.1068/b37092>.

Mahiny, A., Clarke, K., 2013. Simulating hydrologic impacts of urban growth using SLEUTH, multi criteria evaluation and runoff modeling. *J. Environ. Inf.* 22 (1).

Mahiny, A.S., Gholamalifard, M., 2011. Linking SLEUTH Urban Growth Modeling to Multi Criteria Evaluation for a Dynamic Allocation of Sites to Landfill. Paper presented at the Computational Science and Its Applications-ICCSA 2011: International Conference, Santander, Spain, June 20–23, 2011. Proceedings, Part I 11.

Martellozzo, F., Amato, F., Murgante, B., Clarke, K., 2018. Modelling the impact of urban growth on agriculture and natural land in Italy to 2030. *Appl. Geogr.* 91, 156–167.

McGarigal, K., 2015. FRAGSTATS Help. University of Massachusetts, Amherst, MA, USA, p. 182.

Mohammadyari, F., Tavakoli, M., Zarandian, A., Abdollahi, S., 2023. Optimization land use based on multi-scenario simulation of ecosystem service for sustainable landscape planning in a mixed urban - forest watershed. *Ecol. Model.* 483, 110440. <https://doi.org/10.1016/j.ecolmodel.2023.110440>.

Osborne, P.E., Alvares-Sanches, T., 2019. Quantifying how landscape composition and configuration affect urban land surface temperatures using machine learning and neural landscapes. *Comput. Environ. Urban. Syst.* 76, 80–90. <https://doi.org/10.1016/j.compenvurbsys.2019.04.003>.

Ouma, Y., Tjitemisa, T., Segobye, M., Moreri, K., Nkwaeb, B., Maphale, L., Manisa, B., 2021. Urban Land Surface Temperature Variations with LULC, NDVI and NDBI in Semi-Arid Urban Environments: Case Study of Gaborone City, Botswana (1989–2019).

Ozdemir, A., 2011. Using a binary logistic regression method and GIS for evaluating and mapping the groundwater spring potential in the Sultan Mountains (Aksehir, Turkey). *J. Hydrol.* 405 (1–2), 123–136.

Pal, S., Ziaul, S., 2017. Detection of land use and land cover change and land surface temperature in English bazar urban Centre. *Egypt. J. Remote Sens. Space Sci.* 20 (1), 125–145. <https://doi.org/10.1016/j.ejrs.2016.11.003>.

Pande, C.B., Moharir, K.N., Varade, A.M., Abdo, H.G., Mulla, S., Yaseen, Z.M., 2023. Intertwined impacts of urbanization and land cover change on urban climate and agriculture in Aurangabad city (MS), India using google earth engine platform. *J. Clean. Prod.* 422, 138541. <https://doi.org/10.1016/j.jclepro.2023.138541>.

Parvar, Z., Salammahiny, A., 2024. PyLST: a remote sensing application for retrieving land surface temperature (LST) from Landsat data. *Environ. Earth Sci.* 83 (12), 373. <https://doi.org/10.1007/s12665-024-11644-9>.

Parvar, Z., Mohammadzadeh, M., Saeidi, S., 2024a. LCZ framework and landscape metrics: exploration of urban and peri-urban thermal environment emphasizing 2/3D characteristics. *Build. Environ.* 254, 111370. <https://doi.org/10.1016/j.buildenv.2024.111370>.

Parvar, Z., Saeidi, S., Mirkarimi, S., 2024b. Integrating meteorological and geospatial data for forest fire risk assessment. *J. Environ. Manag.* 358, 120925. <https://doi.org/10.1016/j.jenvman.2024.120925>.

Pham, K.T., Lin, T.-H., 2023. Effects of urbanisation on ecosystem service values: A case study of Nha Trang, Vietnam. *Land Use Policy* 128, 106599. <https://doi.org/10.1016/j.landusepol.2023.106599>.

Pokhrel, S., 2019. Green Space Suitability Evaluation for Urban Resilience: An Analysis of Kathmandu Metropolitan City. *Environmental Research Communications, Nepal*, p. 1.

Punia, M., Joshi, P.K., Porwal, M.C., 2011. Decision tree classification of land use land cover for Delhi, India using IRS-P6 AWIFS data. *Expert Syst. Appl.* 38 (5), 5577–5583. <https://doi.org/10.1016/j.eswa.2010.10.078>.

Qiao, Z., Wang, B., Yao, H., Li, Z., Scheu, S., Zhu, Y.-G., Sun, X., 2022. Urbanization and greenspace type as determinants of species and functional composition of collembolan communities. *Geoderma* 428, 116175. <https://doi.org/10.1016/j.geoderma.2022.116175>.

Rafiee, R., Mahiny, A.S., Khorasani, N., Darvishsefat, A.A., Danekar, A., 2009. Simulating urban growth in Mashad City, Iran through the SLEUTH model (UGM). *Cities* 26 (1), 19–26. <https://doi.org/10.1016/j.cities.2008.11.005>.

Rani, S., Mal, S., 2022. Trends in land surface temperature and its drivers over the High Mountain Asia. *Egypt. J. Remote Sens. Space Sci.* 25 (3), 717–729. <https://doi.org/10.1016/j.ejrs.2022.04.005>.

Rienow, A., Goetzke, R., 2015a. Supporting SLEUTH–enhancing a cellular automaton with support vector machines for urban growth modeling. *Comput. Environ. Urban. Syst.* 49, 66–81.

Rienow, A., Goetzke, R., 2015b. Supporting SLEUTH – enhancing a cellular automaton with support vector machines for urban growth modeling. *Comput. Environ. Urban. Syst.* 49, 66–81. <https://doi.org/10.1016/j.compenvurbsys.2014.05.001>.

Riveira, I.S., Maseda, R.C., 2006. A review of rural land-use planning models. *Environ. Plan. B* 33 (2), 165–183. <https://doi.org/10.1068/b31073>.

Rwanga, S., Ndambuki, J., 2017. Accuracy assessment of land use/land cover classification using remote sensing and GIS. *Int. J. Geosci.* 08, 611–622. <https://doi.org/10.4236/ijg.2017.84033>.

Saaty, T.L., 1977. A scaling method for priorities in hierarchical structures. *J. Math. Psychol.* 15 (3), 234–281.

Saeidi, S., Mohammadzadeh, M., Salammahiny, A., Mirkarimi, S.H., 2017. Performance evaluation of multiple methods for landscape aesthetic suitability mapping: a comparative study between multi-criteria evaluation, logistic regression and multi-layer perceptron neural network. *Land Use Policy* 67, 1–12.

Saeidi, S., Mirkarimi, S.H., Mohammadzadeh, M., Salammahiny, A., Arrowsmith, C., 2018. Designing an integrated urban growth prediction model: a scenario-based approach for preserving scenic landscapes. *Geocarto Int.* 33 (12), 1381–1397.

Sakieh, Y., Amiri, B.J., Danekar, A., Feghji, H., Dezhkam, S., 2015. Simulating urban expansion and scenario prediction using a cellular automata urban growth model, SLEUTH, through a case study of Karaj City, Iran. *J. Housing Built Environ.* 30 (4), 591–611. <https://doi.org/10.1007/s10901-014-9432-3>.

Salman Mahiny, A., Gholamalifard, M., 2006. Dynamic spatial modeling of urban growth through cellular automata in a GIS environment. *International. J. Environ. Res. Res. 1 (3)*, 1 (ISSN: 1735-6865).

Salmanmahiny, A., Parvar, Z., Ebrahimonfared, Z., Vesali, F., Donyavi, R., Ramezany, M., Shiadi, N., Rahimy, H., 2022. TOPSIS softwareGorgan University of Agricultural Sciences and Natural Resources. Retrieved from. <https://mte.gau.ac.ir/NewsDetails?newsid=15497>.

Saxena, A., Jat, M.K., 2019. Capturing heterogeneous urban growth using SLEUTH model. *Rem. Sens. Appl.* 13, 426–434. <https://doi.org/10.1016/j.rsase.2018.12.012>.

Saxena, A., Jat, M.K., Clarke, K.C., 2021. Development of SLEUTH-density for the simulation of built-up land density. *Comput. Environ. Urban. Syst.* 86, 101586. <https://doi.org/10.1016/j.compenvurbsys.2020.101586>.

Sharma, R., Pradhan, L., Kumari, M., Bhattacharya, P., 2022. Urban green space planning and development in urban cities using geospatial technology: a case study of Noida. *J. Landsc. Ecol.* 15 (1), 27–46. <https://doi.org/10.2478/jlecol-2022-0002>.

Sharp, R., Tallis, H., Ricketts, T., Guerry, A., Wood, S., Chaplin-Kramer, R., Nelson, E., Ennaanay, D., Wolny, S., Olwero, N., 2018. InVEST 3.7. 0. Post17+hbcb7e191b14 User's Guide. The Natural Capital Project. Stanford University, University of Minnesota.

Song, Z., Li, R., Qiu, R., Liu, S., Tan, C., Li, Q., Ge, W., Han, X., Tang, X., Shi, W., 2018. Global land surface temperature influenced by vegetation cover and PM2. 5 from 2001 to 2016. *Remote Sens.* 10 (12), 2034.

Stumpe, B., Bechtel, B., Heil, J., Jörges, C., Jostrmeier, A., Kalks, F., Schwarz, K., Marschner, B., 2023. Soil texture mediates the surface cooling effect of urban and peri-urban green spaces during a drought period in the city area of Hamburg (Germany). *Sci. Total Environ.* 897, 165228. <https://doi.org/10.1016/j.scitotenv.2023.165228>.

Sun, Y., Shao, Y., 2020. Measuring visitor satisfaction toward peri-urban green and open spaces based on social media data. *Urban For. Urban Green.* 53, 126709. <https://doi.org/10.1016/j.ufug.2020.126709>.

Unal Cilek, M., Cilek, A., 2021. Analyses of land surface temperature (LST) variability among local climate zones (LCZs) comparing Landsat-8 and ENVI-met model data. *Sustain. Cities Soc.* 69, 102877. <https://doi.org/10.1016/j.scs.2021.102877>.

Ustaoglu, E., 2022. *An Assessment of Land Use/Cover Suitable for Peri-urban Green Space Development: an Example of an Integration of GIS with the Multi-Criteria Analysis (MCA) Approach.*

Ustaoglu, E., Aydinoglu, A.C., 2020. Site suitability analysis for green space development of Pendik district (Turkey). *Urban For. Urban Green.* 47, 126542. <https://doi.org/10.1016/j.ufug.2019.126542>.

Varquez, A.C.G., Dong, S., Hanaoka, S., Kanda, M., 2023. Evaluating future railway-induced urban growth of twelve cities using multiple SLEUTH models with open-source geospatial inputs. *Sustain. Cities Soc.* 91, 104442. <https://doi.org/10.1016/j.scs.2023.104442>.

Verdú-Vázquez, A., Fernández-Pablos, E., Lozano-Diez, R.V., López-Zaldívar, Ó., 2021. Green space networks as natural infrastructures in PERI-URBAN areas. *Urban Ecosyst.* 24 (1), 187–204. <https://doi.org/10.1007/s11252-020-01019-w>.

Yang, Q., Li, X., Shi, X., 2008. Cellular automata for simulating land use changes based on support vector machines. *Comput. Geosci.* 34 (6), 592–602.

Yeh, A.G.O., Li, X., Xia, C., 2021. Cellular automata modeling for urban and regional planning. In: Shi, W., Goodchild, M.F., Batty, M., Kwan, M.-P., Zhang, A. (Eds.), *Urban Informatics*. Springer Singapore, Singapore, pp. 865–883.

Yin, H., Kong, F., Hu, Y., James, P., Xu, F., Yu, L., 2016. Assessing growth scenarios for their landscape ecological security impact using the SLEUTH urban growth model. *J. Urban Plan. Dev.* 142 (2), 05015006.

Zarandian, A., Mohammadyari, F., Mirsanjari, M.M., Visockiene, J.S., 2023. Scenario modeling to predict changes in land use/cover using land Change modeler and InVEST model: a case study of Karaj Metropolis, Iran. *Environ. Monit. Assess.* 195 (2), 273. <https://doi.org/10.1007/s10661-022-10740-2>.

Zhao, D., Cai, J., Xu, Y., Liu, Y., Yao, M., 2023. Carbon sinks in urban public green spaces under carbon neutrality: a bibliometric analysis and systematic literature review. *Urban For. Urban Green.* 86, 128037. <https://doi.org/10.1016/j.ufug.2023.128037>.

Zhongming, Z., Linong, L., Xiaona, Y., Wei, L., 2019. *2019 Refinement to the 2006 IPCC Guidelines for National Greenhouse Gas Inventories.*

Žlender, V., Ward Thompson, C., 2017. Accessibility and use of peri-urban green space for inner-city dwellers: a comparative study. *Landsc. Urban Plan.* 165, 193–205. <https://doi.org/10.1016/j.landurbplan.2016.06.011>.